01 Oct 2010

Thermodynamics of Strained Vanadium Dioxide Single Crystals

Yijia Gu
Missouri University of Science and Technology, guyij@mst.edu

Jinbo Cao

Junqiao Wu

Long-Qing Chen

Recommended Citation

Y. Gu et al., "Thermodynamics of Strained Vanadium Dioxide Single Crystals," *Journal of Applied Physics*, vol. 108, no. 8, American Institute of Physics (AIP), Oct 2010.
The definitive version is available at https://doi.org/10.1063/1.3499349

Thermodynamics of strained vanadium dioxide single crystals

Yijia Gu,[1,a)] Jinbo Cao,[2] Junqiao Wu,[2] and Long-Qing Chen[1]
[1]*Department of Materials Science and Engineering, Pennsylvania State University, University Park, Pennsylvania 16802, USA*
[2]*Department of Materials Science and Engineering, University of California, Berkeley, California 97420, USA and Materials Sciences Division, Lawrence Berkeley National Laboratory, Berkeley, California 94720, USA*

(Received 15 July 2010; accepted 3 September 2010; published online 25 October 2010)

Vanadium dioxide undergoes a metal–insulator transition, in which the strain condition plays an important role. To investigate the strain contribution, a phenomenological thermodynamic potential for the vanadium dioxide single crystal was constructed. The transformations under the uniaxial stress, wire, and thin film boundary conditions were analyzed, and the corresponding phase diagrams were constructed. The calculated phase diagrams agree well with existing experimental data, and show that the transformation temperature (and Curie temperature) strongly depends on the strain condition. © *2010 American Institute of Physics*. [doi:10.1063/1.3499349]

I. INTRODUCTION

As a strong correlated material, vanadium dioxide (VO_2) exhibits a metal-insulator transition (MIT) characterized by a first order structural transformation.[1,2] Above the transition temperature, VO_2 has the rutile ($R,P4_2/mnm$) structure and is metallic while below the transition temperature, it has two monoclinic phases, $M1(P2_1/c)$, and $M2(C2/m)$, both of which are insulating.[2] As a promising candidate material for switching devices, VO_2 has been studied for decades.[2]

The MIT is complicated by two possible low temperature monoclinic phases called $M1$ and $M2$. In $M1$ phase, the vanadium atoms form zigzag chains along $[001]_R$ direction while in $M2$, only the vanadium atoms in one sublattice remain zigzag chain; the other half of vanadium atoms are strongly dimerized along the $[001]_R$ direction. $M2$ phase is regarded as a metastable structure of VO_2, and it can only be stabilized by doping,[3–5] or applied stress.[6] Marezio *et al.*[3] revealed that by doping chromium the monoclinic structure is expanded along the $[110]_R$ direction, which stabilizes the $M2$ phase. Pouget *et al.*[6] applied a $[110]_R$ uniaxial stress to a pure VO_2 single crystal and observed a $M1 \rightarrow M2$ phase transformation. By bending the pure VO_2 microbeam along $[001]_R$ direction or taking advantage of substrate mismatch strain, Cao *et al.*[7,8] demonstrated $R \rightarrow M2$ and $M1 \rightarrow M2$ transformations in pure VO_2 nanobeams.

VO_2 is also a promising thermochromic material. Accompanying the abrupt resistivity change, VO_2 undergoes an infrared reflecting state to a relative infrared transparent state change during the MIT. One of the limitations for its chromogenic application is the high transition temperature (341 K).[9] Besides doping, another way to decrease the transition temperature is to use strain. Muraoka *et al.*[10] showed that different substrates (TiO_2 (110) plane and (001) plane) may enormously modify the transition temperature in VO_2 thin films.

As discussed above, strain plays an important role in the MIT of VO_2, including stabilizing the $M2$ phase and modifying the transition temperature of VO_2 thin films. In order to control and manipulate the MIT, it is necessary to understand the thermodynamics of phase transitions under different strain conditions. The primary goal of this paper is to introduce a phenomenological thermodynamic potential, and to calculate the phase diagrams of VO_2 under different strain conditions.

II. THERMODYNAMIC POTENTIAL

Since the structural transformations among R, $M1$, and $M2$ are all of first order, we adopt a six-order Landau polynomial expansion to describe the bulk energy density as a function of order parameters,

$$f_{bulk}(\eta) = \frac{A}{2}(T - T_C)\eta^2 - \frac{B}{4}\eta^4 + \frac{C}{6}\eta^6, \tag{1}$$

where T_C is Curie temperature under the stress-free condition, and A, B, and C are positive constants, η is normalized order parameter describing the R to $M1$ transformation, R to $M2$ transformation, and $M2$ to $M1$ transformation. Take the R to $M1$ transformation for example, at stress-free transformation temperature T_0, the total free energy change is zero, i.e.,

$$\Delta f_{bulk} = f(1) - f(0) = \frac{A}{2}(T_0 - T_C) - \frac{B}{4} + \frac{C}{6}$$
$$= -\Delta H + T_0 \Delta S = 0, \tag{2}$$

where ΔS and ΔH are entropy and enthalpy changes in stress-free R to $M1$ transformation respectively. Hence, we can immediately have

$$\frac{A}{2} = \Delta S = \frac{\Delta H}{T_0}. \tag{3}$$

Similarly, we can use the same method to analyze R to $M2$ and $M2$ to $M1$ transformation.

For the transformation under a stress or fixed strain, the strain energy is given by

[a)]Electronic mail: yug115@psu.edu.

$$f_{elast}(\eta,\varepsilon)=\frac{1}{2}c_{ijkl}(\varepsilon_{ij}-\eta^2\varepsilon_{ij}^0)(\varepsilon_{kl}-\eta^2\varepsilon_{kl}^0), \tag{4}$$

where ε_{ij} is the total strain, ε_{ij}^0 is the stress-free transformation strain, and c_{ijkl} is the elastic stiffness tensor. The total free energy consists of bulk energy and elastic energy, i.e.,

$$\begin{aligned}F(\eta,\varepsilon)&=f_{bulk}(\eta)+f_{elast}(\eta,\varepsilon)\\&=\frac{A}{2}(T-T_C)\eta^2-\frac{B}{4}\eta^4+\frac{C}{6}\eta^6\\&\quad+\frac{1}{2}c_{ijkl}(\varepsilon_{ij}-\eta^2\varepsilon_{ij}^0)(\varepsilon_{kl}-\eta^2\varepsilon_{kl}^0).\end{aligned} \tag{5}$$

As we will show below the elastic energy may strongly change the transformation and Curie temperatures.

III. PHASE DIAGRAMS UNDER DIFFERENT STRAIN CONDITIONS

The strain contributions to the metal-insulator phase transition depend on different mechanical boundary conditions. In this part we will discuss the phase transformations under a uniaxial stress along $[001]_R$ or $[110]_R$ direction, a wire boundary condition, and a thin film boundary condition, respectively.

A. Uniaxial stress

Under a uniaxial stress along the x_3 direction, the thermodynamic potential is the Gibbs free energy, which can be obtained from (5)

$$G=F-\frac{\partial F}{\partial\varepsilon_{ij}}\varepsilon_{ij}=F-\sigma_{ij}\varepsilon_{ij}, \tag{6}$$

where σ_{ij} is applied stress. Minimizing the Gibbs free energy with respect to strain yields

$$\frac{\partial G}{\partial\varepsilon_{ij}}=c_{ijkl}(\varepsilon_{kl}-\eta^2\varepsilon_{kl}^0)-\sigma_{ij}=0. \tag{7}$$

Because all the stress along other directions are equal to zero, e.g., $\sigma_{11}=\sigma_{12}=\sigma_{13}=\sigma_{21}=\sigma_{22}=\sigma_{23}=\sigma_{31}=\sigma_{32}=0$, we have

$$\varepsilon_{33}=\frac{\sigma_{33}}{c_{3333}}+\eta^2\varepsilon_{33}^0. \tag{8}$$

Substituting (7) and (8) back into the Gibbs free energy expression (6), we get

$$\begin{aligned}G(\eta,\sigma)&=\frac{A}{2}\left[(T-T_C)-\frac{2}{A}\sigma_{33}\varepsilon_{33}^0\right]\eta^2-\frac{B}{4}\eta^4+\frac{C}{6}\eta^6\\&\quad-\frac{\sigma_{33}^2}{2c_{3333}}.\end{aligned} \tag{9}$$

From the second-order coefficient of the Gibbs free energy, we can easily get the new Curie temperature

$$T_C'=T_C+\frac{2\sigma_{33}\varepsilon_{33}^0}{A}=T_C+\frac{\sigma_{33}\varepsilon_{33}^0}{\Delta H}T_0. \tag{10}$$

To denote the new transformation and Curie temperatures under stress and strain conditions, we make use of prime sign ($'$), e.g., T_0' is for the new transformation temperature, and T_C' is for the new Curie temperature. The difference between transformation temperature and Curie temperature, ΔT, is a measure of hysteresis which is a characteristic of first order transformations. In order to compare with the experimental data which are all transformation temperatures, we made the following assumption

$$\Delta T=T_0-T_C=T_0'-T_C'. \tag{11}$$

Rearranging (11), we obtain

$$T_0'-T_0=T_C'-T_C. \tag{12}$$

This is a rough assumption which ignores the stress and strain effect on the transformation hysteresis. Besides the elastic property differences between the parent phase and the product phase, the external stress field may affect the thermodynamic hysteresis as well.[11] However, this is not the main purpose of this article. The metastability of hysteresis caused by substrate strain in VO_2 will be investigated in another paper.[12]

With (12), we obtain the new transformation temperature

$$T_0'=T_0\left(1+\frac{\sigma_{33}\varepsilon_{33}^0}{\Delta H}\right). \tag{13}$$

To calculate the transformation temperature under the uniaxial stress condition, we can also apply Clapeyron equation,

$$\frac{d\sigma}{dT_0}=\frac{\Delta H}{\varepsilon^0 T_0}, \tag{14}$$

where σ is applied uniaxial stress, ε^0 is the strain along the same direction as σ, and ΔH is the enthalpy change in stress-free transformation. Integrating from T_0 to T_0' (stress from 0 to σ, correspondingly), we get

$$\sigma=\frac{\Delta H}{\varepsilon^0}\ln\frac{T_0'}{T_0}. \tag{15}$$

If the difference between T_0' and T_0 is small, using Taylor expansion and omitting high order terms, we get

$$T_0'=T_0\left(1+\frac{\varepsilon^0\sigma}{\Delta H}\right). \tag{16}$$

Because ε^0 is the same as ε_{33}^0, and σ is the uniaxial stress along x_3 direction, Eqs. (13) and (16) show essentially the same stress-dependence of transformation temperature T_0'.

As shown in Fig. 1, we can rotate the coordinate system to make $[110]_R$ the new x_3 direction. Thus, we can employ the same formula (13) to analyze the transformation under a uniaxial stress along the $[001]_R$ direction and the $[110]_R$ direction by rotating the transformation strain correspondingly (see Appendix). Although the phase transformations are under two different uniaxial stress directions, the stress-free transformation temperature for $R\rightarrow M1$ remains unchanged at 341 K. With the latent heat for $R\rightarrow M1$ transformation (1025 cal/mol),[13,14] and the latent heat for $M2\rightarrow M1$ transformation (205 cal/mol),[6] we can immediately get the latent

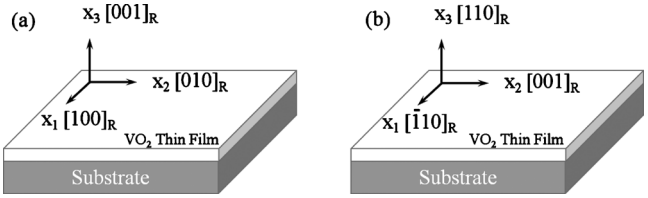

FIG. 1. The transformation of coordinate system. (a) Old coordinate system and (b) new coordinate system. For the $[001]_R$ uniaxial stress condition, and $(001)_R$ VO_2 thin film condition, we use the old coordinate system (a). For the $[110]_R$ uniaxial stress condition, wire condition, and $(110)_R$ VO_2 thin film condition, we adopt the new coordinate system (b).

heat for $R \rightarrow M2$ transformation (820 cal/mol). Therefore, taking 0.01GPa as the minimum stress to induce $M2$,[6] we can calculate the stress-free transformation temperatures for $R \rightarrow M2$ and $M1 \rightarrow M2$, and consequently construct temperature versus uniaxial stress phase diagrams for pure VO_2. The calculated minimum stress to induce $M2$ phase (the stress of the triple point) under uniaxial stress along $[001]_R$ direction is 0.014 GPa, the stress-free transformation temperatures for $R \rightarrow M2$ and $M1 \rightarrow M2$ are 340.7 K and 342.0 K, respectively.

The calculated phase diagram of $[110]_R$ uniaxial stress agrees well with the experimental data (Fig. 2). As shown in Appendix, the transformation strain ε_{33}^0 in the new coordinate system has two different values due to different variants. So we selected the variant which has a lower free energy under tensile stress to construct the diagram. However, the calculated diagram of $[001]_R$ uniaxial stress deviates from the measured data under tensile stresses. During the $M1 \rightarrow M2$ transformation under $[110]_R$ uniaxial stress, a transitional triclinic phase (T) was observed.[6] Such a transitional phase was not taken into account in our thermodynamic analysis. The $T \rightarrow M2$ transformation is of first order but $M1 \rightarrow T$ is not or very weak first order transformation with no observable latent heat.[4] Because the continuous change in $M1 \rightarrow T$ transformation, the transformation strain ε^0 of $T \rightarrow M2$ may be smaller than that of $M1 \rightarrow M2$ under the $[001]_R$ uniaxial stress. Therefore, the measured critical $[001]_R$ uniaxial stress, which may be of $T \rightarrow M2$, is larger

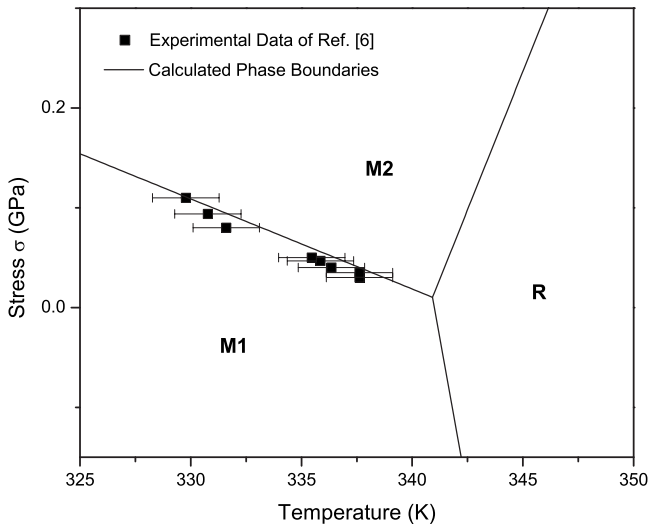

FIG. 2. $[110]_R$ uniaxial stress vs transformation temperature in VO_2 single crystal.

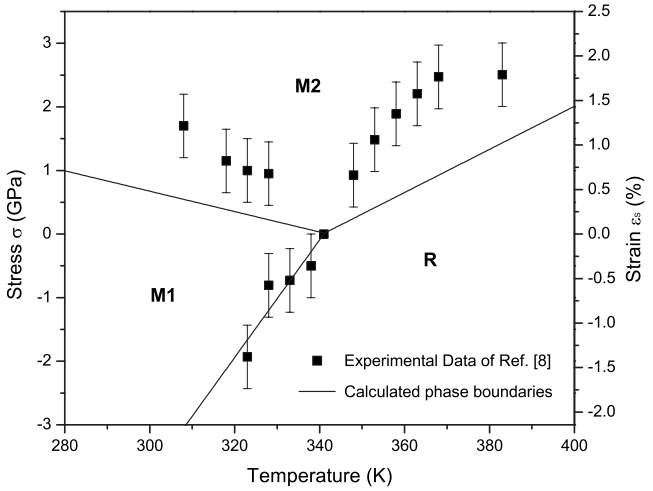

FIG. 3. $[001]_R$ uniaxial stress (or mismatch strain of wire with longitudinal direction of $[001]_R$) vs transformation temperature in VO_2 single crystal. The solid lines are calculated phase boundaries. For experiment condition of Ref. 8, the Young's modulus should be smaller due to the surface effect. Lack of the actual value of Young's modulus, we adopted 140 GPa (Ref. 18) to calculate the mismatch strain ε_S.

than our calculation for $M1 \rightarrow M2$. But this explanation cannot be applied to the difference of $R \rightarrow M2$ transformation in Fig. 3 and the well agreement of $M1 \rightarrow M2$ under $[110]_R$ uniaxial stress in Fig. 2.

Another possibility which may account for the deviation of Fig. 3 arises from the surface stress of the nanobeams in the experiments. Due to the large surface area of $(110)_R$ side planes, the surface stress along $[001]_R$ direction may be quite large. Sohn *et al.*[15] reported that the surface stress could stabilize $M2$ phase in suspended pure VO_2 nanowires. The surface tensile stress is therefore comparable to the critical stress. For the transformation under the $[110]_R$ uniaxial stress, the experiment samples were VO_2 single crystals with dimensions 0.5 $mm^2 \times 2$ mm and 3 $mm^2 \times 4$ mm.[6] So there is no such strong surface stress caused by the special geometry of nanobeam.

B. Wire boundary condition

If the longitudinal direction of a wire is along $x_2[001]_R$ as shown in Fig. 1(b), all the stress components associated with x_1 and x_3 directions are zero, i.e.,

$$\sigma_{11} = \sigma_{12} = \sigma_{13} = \sigma_{21} = \sigma_{23} = \sigma_{31} = \sigma_{32} = \sigma_{33} = 0,$$
$$\text{and} \quad \varepsilon_{22} = \varepsilon_S, \tag{17}$$

where ε_S is the mismatch strain. This wire boundary condition is essentially the same as the $[001]_R$ uniaxial stress case because the strain or stress is only along the $[001]_R$ direction, and all the other directions are stress-free. To satisfy the above stress and strain boundary condition, it can be immediately shown that

$$\frac{\partial F}{\partial \varepsilon_{ij}} = c_{ijkl}(\varepsilon_{kl} - \eta^2 \varepsilon_{kl}^0) = \sigma_{ij} = 0$$
$$(ij = 11,12,13,21,23,31,32,33). \tag{18}$$

So we have

$$\begin{cases} \sigma_{11} = c_{1111}(\varepsilon_{11} - \eta^2\varepsilon_{11}^0) + c_{1122}(\varepsilon_{22} - \eta^2\varepsilon_{22}^0) + c_{1133}(\varepsilon_{33} - \eta^2\varepsilon_{33}^0) = 0 \\ \sigma_{33} = c_{3311}(\varepsilon_{11} - \eta^2\varepsilon_{11}^0) + c_{3322}(\varepsilon_{22} - \eta^2\varepsilon_{22}^0) + c_{3333}(\varepsilon_{33} - \eta^2\varepsilon_{33}^0) = 0 \end{cases}. \tag{19}$$

Solving (19) with $c_{1133}=c_{3311}$, $c_{3333}=c_{1111}$, and $c_{1122}=c_{3322}$ (symmetry of elastic stiffness constants for tetragonal phase, see Eq. (A8) in Appendix), we get

$$\varepsilon_{11} - \eta^2\varepsilon_{11}^0 = \varepsilon_{33} - \eta^2\varepsilon_{33}^0 = -\frac{c_{1122}}{c_{1111}+c_{1133}}(\varepsilon_{22} - \eta^2\varepsilon_{22}^0). \tag{20}$$

Substituting (18) and (20) into (4), we get the elastic energy

$$\begin{aligned} f_{elast} &= \frac{1}{2}\sigma_{ij}(\varepsilon_{ij} - \eta^2\varepsilon_{ij}^0) = \frac{1}{2}c_{22kl}(\varepsilon_{kl} - \eta^2\varepsilon_{kl}^0)(\varepsilon_{22} - \eta^2\varepsilon_{22}^0) \\ &= \frac{1}{2}(\varepsilon_{22} - \eta^2\varepsilon_{22}^0)[c_{2211}(\varepsilon_{11} - \eta^2\varepsilon_{11}^0) + c_{2222}(\varepsilon_{22} \\ &\quad - \eta^2\varepsilon_{22}^0) + c_{2233}(\varepsilon_{33} - \eta^2\varepsilon_{33}^0)] \\ &= \frac{1}{2}(\varepsilon_{22} - \eta^2\varepsilon_{22}^0)^2\left(c_{2222} - \frac{2c_{1122}^2}{c_{1111}+c_{1133}}\right). \end{aligned} \tag{21}$$

Using the Voigt's notation, the total free energy (5) is given by

$$\begin{aligned} F &= \left[\frac{A}{2}(T - T_C) - \left(c_{22} - \frac{2c_{12}^2}{c_{11}+c_{13}}\right)\varepsilon_2^0\varepsilon_S\right]\eta^2 \\ &\quad - \left[\frac{B}{4} - \frac{(\varepsilon_2^0)^2}{2}\left(c_{22} - \frac{2c_{12}^2}{c_{11}+c_{13}}\right)\right]\eta^4 + \frac{C}{6}\eta^6 \\ &\quad + \frac{\varepsilon_S^2}{2}\left(c_{22} - \frac{2c_{12}^2}{c_{11}+c_{13}}\right), \end{aligned} \tag{22}$$

in which only the second-order coefficient depends on the mismatch strain, and the new Curie temperature is given by

$$\begin{aligned} T_C' &= T_C + \frac{2\varepsilon_2^0}{A}\left(c_{22} - \frac{2c_{12}^2}{c_{11}+c_{13}}\right)\varepsilon_S \\ &= T_C + \frac{T_0\varepsilon_2^0}{\Delta H}\left(c_{22} - \frac{2c_{12}^2}{c_{11}+c_{13}}\right)\varepsilon_S. \end{aligned} \tag{23}$$

Plugging (12) in (23), we obtain the new transformation temperature

$$T_0' = T_0\left[1 + \frac{\varepsilon_2^0}{\Delta H}\left(c_{22} - \frac{2c_{12}^2}{c_{11}+c_{13}}\right)\varepsilon_S\right]. \tag{24}$$

If the elastic constant is isotropic, e.g., $c_{12}=c_{13}$, $c_{11}=c_{22}$, we get

$$T_0' = T_0\left[1 + \frac{\varepsilon_2^0}{\Delta H}\left(c_{11} - \frac{2c_{12}^2}{c_{11}+c_{12}}\right)\varepsilon_S\right] = T_0\left(1 + \frac{\varepsilon_2^0}{\Delta H}E\varepsilon_S\right), \tag{25}$$

where E is Young's modulus along $[001]_R$ direction (x_2 direction of the new coordinate system). Because ε_2^0 is the strain along the longitudinal direction, this result has the same form as our result (13) for a uniaxial stress along the $[001]_R$ direction.

The phase transitions in VO_2 nanowires have been studied experimentally. Wu and co-workers[8,16] took advantage of different substrate mismatch strains and produced a self-organized metal-insulator domain structure pattern. This one-dimensional alternating domain structure is further complicated by polysynthetic $M2$ twins along the width direction.[8] Jones *et al.*[17] also observed complicated domain pattern in pure VO_2 nanowires, and summarized two transformation sequences, e.g., $M1 \rightarrow M1+R \rightarrow M2+R \rightarrow R$, and $M2 \rightarrow M2+R \rightarrow R$. These two transformation paths are mainly caused by different substrate tensile strains. As shown in Fig. 3, if the substrate mismatch strain value is below the $M2-M1$ phase boundary, the transformation may follow the first path; while if the strain value is above the $M2-M1$ phase boundary, it follows the latter one.

C. Thin film boundary condition

The thin film boundary condition is a mixed set of strain and stress boundary conditions. As shown in Fig. 1, the film is clamped on the substrate in x_1-x_2 plane but is stress-free along the x_3 direction. So there is a biaxial strain in the x_1-x_2 plane, and all the stress components associated with the x_3 direction are equal to zero, i.e.,

$$\begin{aligned} &\varepsilon_{11} = \varepsilon_{22} = \varepsilon_S, \quad \varepsilon_{12} = \varepsilon_{21} = 0, \\ &\text{and} \quad \sigma_{13} = \sigma_{23} = \sigma_{31} = \sigma_{32} = \sigma_{33} = 0, \end{aligned} \tag{26}$$

where ε_S is the mismatch strain.

To satisfy the above stress-free condition, it requires that

$$\frac{\partial F}{\partial \varepsilon_{ij}} = c_{ijkl}(\varepsilon_{kl} - \eta^2\varepsilon_{kl}^0) = 0 \quad (ij = 13,31,23,32,33). \tag{27}$$

So we have

$$\begin{aligned} \sigma_{11} &= \left(c_{1111} - \frac{c_{3311}^2}{c_{3333}}\right)(\varepsilon_S - \eta^2\varepsilon_{11}^0) \\ &\quad + \left(c_{1122} - \frac{c_{1133}c_{3322}}{c_{3333}}\right)(\varepsilon_S - \eta^2\varepsilon_{22}^0), \end{aligned} \tag{28a}$$

$$\begin{aligned} \sigma_{22} &= \left(c_{2211} - \frac{c_{2233}c_{3311}}{c_{3333}}\right)(\varepsilon_S - \eta^2\varepsilon_{11}^0) \\ &\quad + \left(c_{2222} - \frac{c_{3322}^2}{c_{3333}}\right)(\varepsilon_S - \eta^2\varepsilon_{22}^0), \end{aligned} \tag{28b}$$

$$\sigma_{12} = \sigma_{21} = 2c_{1212}(\varepsilon_{12} - \eta^2\varepsilon_{12}^0) = -2c_{1212}\eta^2\varepsilon_{12}^0. \tag{28c}$$

With (27) and the thin film boundary condition (26), we get

$$f_{elast} = \frac{1}{2}\sigma_{ij}(\varepsilon_{ij} - \eta^2\varepsilon_{ij}^0)$$

$$= \frac{1}{2}[\sigma_{11}(\varepsilon_S - \eta^2\varepsilon_{11}^0) + \sigma_{22}(\varepsilon_S - \eta^2\varepsilon_{22}^0) - 2\sigma_{12}\eta^2\varepsilon_{12}^0]. \quad (29)$$

Substituting (28a)–(28c) in (29) and following Voigt's notation, we obtain the elastic energy

$$f_{elast} = \frac{1}{2}\left(c_{11} - \frac{c_{13}^2}{c_{33}}\right)(\varepsilon_S - \eta^2\varepsilon_1^0)^2 + \frac{1}{2}\left(c_{22} - \frac{c_{23}^2}{c_{33}}\right)(\varepsilon_S - \eta^2\varepsilon_2^0)^2 + \left(c_{12} - \frac{c_{23}c_{13}}{c_{33}}\right)(\varepsilon_S - \eta^2\varepsilon_1^0)(\varepsilon_S - \eta^2\varepsilon_2^0) + \frac{c_{66}}{2}(\eta^2\varepsilon_6^0)^2. \quad (30)$$

Thus, substituting (30) in (5), we obtain the free energy under thin film boundary condition

$$F = \left[\frac{A}{2}(T - T_C) - \frac{c_{33}(c_{11} + c_{12}) - c_{13}(c_{13} + c_{23})}{c_{33}}\varepsilon_1^0\varepsilon_S - \frac{c_{33}(c_{12} + c_{22}) - c_{23}(c_{13} + c_{23})}{c_{33}}\varepsilon_2^0\varepsilon_S\right]\eta^2 - \left[\frac{B}{4} - \frac{c_{33}c_{11} - c_{13}^2}{2c_{33}}(\varepsilon_1^0)^2 - \frac{c_{22}c_{33} - c_{23}^2}{2c_{33}}(\varepsilon_2^0)^2 - \frac{c_{12}c_{33} - c_{23}c_{13}}{c_{33}}\varepsilon_1^0\varepsilon_2^0 - \frac{c_{66}}{2}(\varepsilon_6^0)^2\right]\eta^4 + \frac{C}{6}\eta^6 + \frac{c_{33}(c_{11} + c_{22} + 2c_{12}) - (c_{13} + c_{23})^2}{2c_{33}}\varepsilon_S^2. \quad (31)$$

Similarly, with the Curie–Weiss law, we obtain the new Curie temperature

$$T_C' = T_C + \frac{T_0\varepsilon_S}{\Delta H}\left[\frac{c_{33}(c_{11} + c_{12}) - c_{13}(c_{13} + c_{23})}{c_{33}}\varepsilon_1^0 + \frac{c_{33}(c_{12} + c_{22}) - c_{23}(c_{13} + c_{23})}{c_{33}}\varepsilon_2^0\right]. \quad (32)$$

With (12), we get the new transformation temperature

$$T_0' = T_0 + \frac{T_0\varepsilon_S}{\Delta H}\left[\frac{c_{33}(c_{11} + c_{12}) - c_{13}(c_{13} + c_{23})}{c_{33}}\varepsilon_1^0 + \frac{c_{33}(c_{12} + c_{22}) - c_{23}(c_{13} + c_{23})}{c_{33}}\varepsilon_2^0\right]. \quad (33)$$

For isotropic elastic constants, $c_{12}=c_{13}=c_{23}$, $c_{11}=c_{22}=c_{33}$. Then, we get

$$T_0' = T_0 + \frac{T_0(\varepsilon_1^0 + \varepsilon_2^0)}{\Delta H}\frac{c_{11}(c_{11} + c_{12}) - 2c_{12}^2}{c_{11}}\varepsilon_S = T_0\left[1 + \frac{(\varepsilon_1^0 + \varepsilon_2^0)}{\Delta H}\frac{E}{1 - \nu}\varepsilon_S\right], \quad (34)$$

where E is Young's modulus for VO_2 thin film and ν is Poisson ratio. Taking the value of E to be 140 GPa,[18] and ν to be 0.3, we can construct the phase diagram of $R \rightarrow M1$ for $(001)_R$ VO_2 thin films and $(110)_R$ VO_2 thin films. As shown in Fig. 4, the constructed phase diagram agrees qualitatively with the experimental results. The transformation temperature decreases with mismatch strain in $(001)_R$ VO_2 thin films, while increases with mismatch strain in $(110)_R$ VO_2 thin films. The deviation may arise from the anisotropic elastic constants of the thin film.

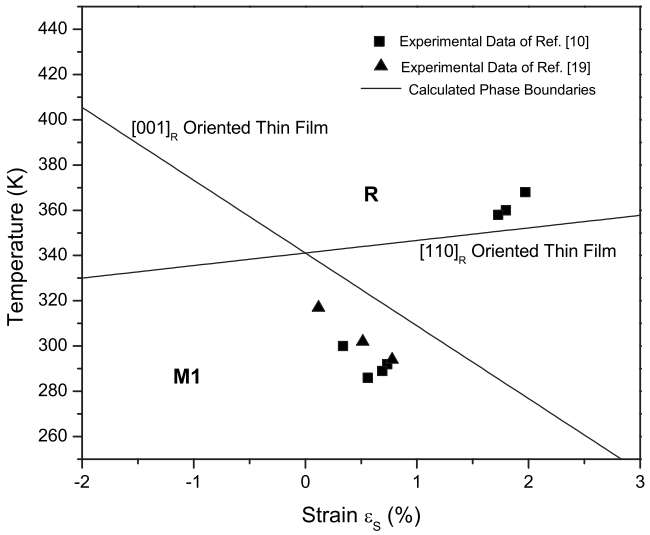

FIG. 4. Transformation temperature as a function of mismatch strain for $(001)_R$ VO_2 thin film and $(110)_R$ VO_2 thin film. The experimental mismatch strain values of $(110)_R$ VO_2 thin film on the (110) oriented TiO_2 substrate was directly calculated from the c values of Ref. 10. Because there are only experimental c values for the $(001)_R$ VO_2 thin film on the (001) oriented TiO_2 substrate (Refs. 10 and 19), we employed the relation $\Delta a_M = -2\Delta b_M$ (Ref. 20) to calculate the mismatch strain.

IV. CONCLUSIONS

A sixth-order polynomial thermodynamic potential is presented for VO_2 single crystals. With this potential, the transformation temperature as a function of different strain conditions are calculated, and the computed phase diagrams agree well with experimental data. The calculated minimum uniaxial stress to induce $M2$ phase is about 0.014 GPa, indicating that the free energy difference between $M1$ and $M2$ phase is very small. The mechanical boundary conditions can greatly modify the transformation temperature, and the results can potentially be employed to guide experiments to obtain the desired phases and transition temperatures using strains.

ACKNOWLEDGMENTS

This work is supported by NSF under Grant No. DMR 0507146.

APPENDIX

Comparing the lattice parameters for VO_2,[3,21–24] we took the following lattice parameters for R, $M1$, and $M2$ phase in our calculation (Table I).

Using these lattice parameters, we get the transformation strains for the four variants of $R \rightarrow M1$ transformation

TABLE I. Lattice parameters of VO_2 taken in this paper.

R		$M1$				$M2$			
$a_R(=b_R)$ (Å)	c_R (Å)	a_M (Å)	b_M (Å)	c_M (Å)	β (°)	a_M (Å)	b_M (Å)	c_M (Å)	β (°)
4.5546	2.8521	5.7474	4.5274	5.3788	122.63	9.0632	5.7985	4.5236	91.865

$$\varepsilon_1=\begin{pmatrix}\varepsilon_{11}&0&\varepsilon_{13}\\0&\varepsilon_{22}&0\\\varepsilon_{13}&0&\varepsilon_{33}\end{pmatrix},\quad \varepsilon_2=\begin{pmatrix}\varepsilon_{22}&0&0\\0&\varepsilon_{11}&\varepsilon_{13}\\0&\varepsilon_{13}&\varepsilon_{33}\end{pmatrix},$$

$$\varepsilon_3=\begin{pmatrix}\varepsilon_{11}&0&-\varepsilon_{13}\\0&\varepsilon_{22}&0\\-\varepsilon_{13}&0&\varepsilon_{33}\end{pmatrix},\quad \varepsilon_4=\begin{pmatrix}\varepsilon_{22}&0&0\\0&\varepsilon_{11}&-\varepsilon_{13}\\0&-\varepsilon_{13}&\varepsilon_{33}\end{pmatrix}, \tag{A1}$$

where $\varepsilon_{11}=-0.005\,403\,12$, $\varepsilon_{22}=-0.005\,954\,15$, $\varepsilon_{33}=0.007\,636\,22$, $\varepsilon_{13}=-0.004\,612\,24$.

Transformed to the new coordinate system [Fig. 1(b)], the transformation strains of $M1$ phase become

$$\varepsilon_1=\begin{pmatrix}\frac{\varepsilon_{11}+\varepsilon_{22}}{2}&-\frac{\varepsilon_{13}}{\sqrt{2}}&\frac{\varepsilon_{22}-\varepsilon_{11}}{2}\\-\frac{\varepsilon_{13}}{\sqrt{2}}&\varepsilon_{33}&\frac{\varepsilon_{13}}{\sqrt{2}}\\\frac{\varepsilon_{22}-\varepsilon_{11}}{2}&\frac{\varepsilon_{13}}{\sqrt{2}}&\frac{\varepsilon_{11}+\varepsilon_{22}}{2}\end{pmatrix},$$

$$\varepsilon_2=\begin{pmatrix}\frac{\varepsilon_{11}+\varepsilon_{22}}{2}&\frac{\varepsilon_{13}}{\sqrt{2}}&\frac{\varepsilon_{11}-\varepsilon_{22}}{2}\\\frac{\varepsilon_{13}}{\sqrt{2}}&\varepsilon_{33}&\frac{\varepsilon_{13}}{\sqrt{2}}\\\frac{\varepsilon_{11}-\varepsilon_{22}}{2}&\frac{\varepsilon_{13}}{\sqrt{2}}&\frac{\varepsilon_{11}+\varepsilon_{22}}{2}\end{pmatrix},$$

$$\varepsilon_3=\begin{pmatrix}\frac{\varepsilon_{11}+\varepsilon_{22}}{2}&\frac{\varepsilon_{13}}{\sqrt{2}}&\frac{\varepsilon_{22}-\varepsilon_{11}}{2}\\\frac{\varepsilon_{13}}{\sqrt{2}}&\varepsilon_{33}&-\frac{\varepsilon_{13}}{\sqrt{2}}\\\frac{\varepsilon_{22}-\varepsilon_{11}}{2}&-\frac{\varepsilon_{13}}{\sqrt{2}}&\frac{\varepsilon_{11}+\varepsilon_{22}}{2}\end{pmatrix},$$

$$\varepsilon_4=\begin{pmatrix}\frac{\varepsilon_{11}+\varepsilon_{22}}{2}&-\frac{\varepsilon_{13}}{\sqrt{2}}&\frac{\varepsilon_{11}-\varepsilon_{22}}{2}\\-\frac{\varepsilon_{13}}{\sqrt{2}}&\varepsilon_{33}&-\frac{\varepsilon_{13}}{\sqrt{2}}\\\frac{\varepsilon_{11}-\varepsilon_{22}}{2}&-\frac{\varepsilon_{13}}{\sqrt{2}}&\frac{\varepsilon_{11}+\varepsilon_{22}}{2}\end{pmatrix}. \tag{A2}$$

Similarly, we get the transformation strains for the four variants of $M2$ phase,

$$\varepsilon_1=\begin{pmatrix}\varepsilon_{11}&\varepsilon_{12}&0\\\varepsilon_{12}&\varepsilon_{22}&0\\0&0&\varepsilon_{33}\end{pmatrix},\quad \varepsilon_2=\begin{pmatrix}\varepsilon_{11}&-\varepsilon_{12}&0\\-\varepsilon_{12}&\varepsilon_{22}&0\\0&0&\varepsilon_{33}\end{pmatrix},$$

$$\varepsilon_3=\begin{pmatrix}\varepsilon_{22}&\varepsilon_{12}&0\\\varepsilon_{12}&\varepsilon_{11}&0\\0&0&\varepsilon_{33}\end{pmatrix},\quad \varepsilon_4=\begin{pmatrix}\varepsilon_{22}&-\varepsilon_{12}&0\\-\varepsilon_{12}&\varepsilon_{11}&0\\0&0&\varepsilon_{33}\end{pmatrix}, \tag{A3}$$

where $\varepsilon_{11}=-0.005\,561\,33$, $\varepsilon_{22}=-0.006\,258\,90$, $\varepsilon_{33}=0.016\,668\,3$, $\varepsilon_{12}=-0.016\,099\,9$.

Transformed to the new coordinate system [Fig. 1(b)], the transformation strains of $R\rightarrow M2$ become

$$\varepsilon_1=\begin{pmatrix}\frac{\varepsilon_{11}+\varepsilon_{22}}{2}-\varepsilon_{12}&&\frac{\varepsilon_{22}-\varepsilon_{11}}{2}\\&\varepsilon_{33}&\\\frac{\varepsilon_{22}-\varepsilon_{11}}{2}&&\frac{\varepsilon_{11}+\varepsilon_{22}}{2}+\varepsilon_{12}\end{pmatrix},$$

$$\varepsilon_2=\begin{pmatrix}\frac{\varepsilon_{11}+\varepsilon_{22}}{2}+\varepsilon_{12}&&\frac{\varepsilon_{22}-\varepsilon_{11}}{2}\\&\varepsilon_{33}&\\\frac{\varepsilon_{22}-\varepsilon_{11}}{2}&&\frac{\varepsilon_{11}+\varepsilon_{22}}{2}-\varepsilon_{12}\end{pmatrix},$$

$$\varepsilon_3=\begin{pmatrix}\frac{\varepsilon_{11}+\varepsilon_{22}}{2}-\varepsilon_{12}&&\frac{\varepsilon_{11}-\varepsilon_{22}}{2}\\&\varepsilon_{33}&\\\frac{\varepsilon_{11}-\varepsilon_{22}}{2}&&\frac{\varepsilon_{11}+\varepsilon_{22}}{2}+\varepsilon_{12}\end{pmatrix},$$

$$\varepsilon_4=\begin{pmatrix}\frac{\varepsilon_{11}+\varepsilon_{22}}{2}+\varepsilon_{12}&&\frac{\varepsilon_{11}-\varepsilon_{22}}{2}\\&\varepsilon_{33}&\\\frac{\varepsilon_{11}-\varepsilon_{22}}{2}&&\frac{\varepsilon_{11}+\varepsilon_{22}}{2}-\varepsilon_{12}\end{pmatrix}. \tag{A4}$$

The transformation strains for $M2\rightarrow M1$ are

$$\varepsilon_1=\begin{pmatrix}\varepsilon_{11}&\varepsilon_{12}&0\\\varepsilon_{12}&\varepsilon_{22}&\varepsilon_{23}\\0&\varepsilon_{23}&\varepsilon_{33}\end{pmatrix},\quad \varepsilon_2=\begin{pmatrix}\varepsilon_{11}&\varepsilon_{12}&0\\\varepsilon_{12}&\varepsilon_{22}&-\varepsilon_{23}\\0&-\varepsilon_{23}&\varepsilon_{33}\end{pmatrix},$$

$$\varepsilon_3 = \begin{pmatrix} \varepsilon_{11} & -\varepsilon_{12} & 0 \\ -\varepsilon_{12} & \varepsilon_{22} & -\varepsilon_{23} \\ 0 & -\varepsilon_{23} & \varepsilon_{33} \end{pmatrix}, \quad \varepsilon_4 = \begin{pmatrix} \varepsilon_{11} & -\varepsilon_{12} & 0 \\ -\varepsilon_{12} & \varepsilon_{22} & \varepsilon_{23} \\ 0 & \varepsilon_{23} & \varepsilon_{33} \end{pmatrix}, \tag{A5}$$

where $\varepsilon_{11}=-0.000\,397\,239$, $\varepsilon_{22}=0.001\,930\,03$, $\varepsilon_{33}=-0.008\,740\,72$, $\varepsilon_{12}=0.016\,288\,1$, $\varepsilon_{23}=-0.004\,568\,32$.

Transformed to the new coordinate system [Fig. 1(b)], the transformation strains of $M2 \rightarrow M1$ become

$$\varepsilon_1 = \begin{pmatrix} \frac{\varepsilon_{11}+\varepsilon_{22}}{2} - \varepsilon_{12} & \frac{\varepsilon_{23}}{\sqrt{2}} & \frac{\varepsilon_{22}-\varepsilon_{11}}{2} \\ \frac{\varepsilon_{23}}{\sqrt{2}} & \varepsilon_{33} & \frac{\varepsilon_{23}}{\sqrt{2}} \\ \frac{\varepsilon_{22}-\varepsilon_{11}}{2} & \frac{\varepsilon_{23}}{\sqrt{2}} & \frac{\varepsilon_{11}+\varepsilon_{22}}{2} + \varepsilon_{12} \end{pmatrix},$$

$$\varepsilon_2 = \begin{pmatrix} \frac{\varepsilon_{11}+\varepsilon_{22}}{2} - \varepsilon_{12} & -\frac{\varepsilon_{23}}{\sqrt{2}} & \frac{\varepsilon_{22}-\varepsilon_{11}}{2} \\ -\frac{\varepsilon_{23}}{\sqrt{2}} & \varepsilon_{33} & -\frac{\varepsilon_{23}}{\sqrt{2}} \\ \frac{\varepsilon_{22}-\varepsilon_{11}}{2} & -\frac{\varepsilon_{23}}{\sqrt{2}} & \frac{\varepsilon_{11}+\varepsilon_{22}}{2} + \varepsilon_{12} \end{pmatrix},$$

$$\varepsilon_3 = \begin{pmatrix} \frac{\varepsilon_{11}+\varepsilon_{22}}{2} + \varepsilon_{12} & -\frac{\varepsilon_{23}}{\sqrt{2}} & \frac{\varepsilon_{22}-\varepsilon_{11}}{2} \\ -\frac{\varepsilon_{23}}{\sqrt{2}} & \varepsilon_{33} & -\frac{\varepsilon_{23}}{\sqrt{2}} \\ \frac{\varepsilon_{22}-\varepsilon_{11}}{2} & -\frac{\varepsilon_{23}}{\sqrt{2}} & \frac{\varepsilon_{11}+\varepsilon_{22}}{2} - \varepsilon_{12} \end{pmatrix},$$

$$\varepsilon_4 = \begin{pmatrix} \frac{\varepsilon_{11}+\varepsilon_{22}}{2} + \varepsilon_{12} & \frac{\varepsilon_{23}}{\sqrt{2}} & \frac{\varepsilon_{22}-\varepsilon_{11}}{2} \\ \frac{\varepsilon_{23}}{\sqrt{2}} & \varepsilon_{33} & \frac{\varepsilon_{23}}{\sqrt{2}} \\ \frac{\varepsilon_{22}-\varepsilon_{11}}{2} & \frac{\varepsilon_{23}}{\sqrt{2}} & \frac{\varepsilon_{11}+\varepsilon_{22}}{2} - \varepsilon_{12} \end{pmatrix}. \tag{A6}$$

Typical elastic stiffness constants for tetragonal phase (class $4/mmm$)

$$\begin{pmatrix} c_{11} & c_{12} & c_{13} & & & \\ c_{12} & c_{11} & c_{13} & & & \\ c_{13} & c_{13} & c_{33} & & & \\ & & & c_{44} & & \\ & & & & c_{44} & \\ & & & & & c_{66} \end{pmatrix}. \tag{A7}$$

Transformed to the new coordinate system, it becomes

$$\begin{pmatrix} \frac{c_{11}+c_{12}}{2} + c_{66} & c_{13} & \frac{c_{11}+c_{12}}{2} - c_{66} & & & \\ c_{13} & c_{33} & c_{13} & & & \\ \frac{c_{11}+c_{12}}{2} - c_{66} & c_{13} & \frac{c_{11}+c_{12}}{2} + c_{66} & & & \\ & & & c_{44} & & \\ & & & & \frac{c_{11}-c_{12}}{2} & \\ & & & & & c_{44} \end{pmatrix}. \tag{A8}$$

[1] F. J. Morin, Phys. Rev. Lett. **3**, 34 (1959).
[2] V. Eyert, Ann. Phys. **11**, 650 (2002).
[3] M. Marezio, B. Mcwhan, P. D. Dernier, and J. P. Remeika, Phys. Rev. B **5**, 2541 (1972).
[4] J. P. Pouget, H. Launois, T. M. Rice, P. Dernier, A. Gossard, G. Villeneu, and P. Hagenmul, Phys. Rev. B **10**, 1801 (1974).
[5] J. M. Booth and P. S. Casey, Phys. Rev. Lett. **103**, 086402 (2009).
[6] J. P. Pouget, H. Launois, J. P. Dhaenens, P. Merenda, and T. M. Rice, Phys. Rev. Lett. **35**, 873 (1975).
[7] J. Cao, E. Ertekin, V. Srinivasan, W. Fan, S. Huang, H. Zheng, J. W. L. Yim, D. R. Khanal, D. F. Ogletree, J. C. Grossmanan, and J. Wu, Nat. Nanotechnol. **4**, 732 (2009).
[8] J. Cao, Y. Gu, W. Fan, L. Q. Chen, D. F. Ogletree, K. Chen, N. Tamura, M. Kunz, C. Barrett, J. Seidel, and J. Wu, Nano Lett. **10**, 2667 (2010).
[9] C. G. Granqvist, Sol. Energy Mater. Sol. Cells **91**, 1529 (2007).
[10] Y. Muraoka, Y. Ueda, and Z. Hiroi, J. Phys. Chem. Solids **63**, 965 (2002).
[11] A. Roytburd and J. Slutsker, Physica B **233**, 390 (1997).
[12] W. Fan, J. Cao, J. Seidel, Y. Gu, J. W. Yim, C. Barrett, K. M. Yu, L. Q. Chen, and J. Wu, (unpublished).
[13] O. A. Cook, J. Am. Chem. Soc. **69**, 331 (1947).
[14] C. N. Berglund and H. Guggenhe, Phys. Rev. **185**, 1022 (1969).
[15] J. I. Sohn, H. J. Joo, D. Ahn, H. H. Lee, A. E. Porter, K. Kim, D. J. Kang, and M. E. Welland, Nano Lett. **9**, 3392 (2009).
[16] J. Q. Wu, Q. Gu, B. S. Guiton, N. P. de Leon, O. Y. Lian, and H. Park, Nano Lett. **6**, 2313 (2006).
[17] A. C. Jones, S. Berweger, J. Wei, D. Cobden, and M. B. Raschke, Nano Lett. **10**, 1574 (2010).
[18] K. Y. Tsai, T. S. Chin, and H. P. D. Shieh, Jpn. J. Appl. Phys., Part 1 **43**, 6268 (2004).
[19] K. Nagashima, T. Yanagida, H. Tanaka, and T. Kawai, J. Appl. Phys. **101**, 026103 (2007).
[20] J. C. Rakotoniaina, R. Mokranitamellin, J. R. Gavarri, G. Vacquier, A. Casalot, and G. Calvarin, J. Solid State Chem. **103**, 81 (1993).
[21] G. Andersson, Acta Chem. Scand. **10**, 623 (1956).
[22] J. M. Longo and P. Kierkegaard, Acta Chem. Scand. **24**, 420 (1970).
[23] D. B. McWhan, M. Marezio, J. P. Remeika, and P. D. Dernier, Phys. Rev. B **10**, 490 (1974).
[24] M. Ghedira, H. Vincent, M. Marezio, and J. C. Launay, J. Solid State Chem. **22**, 423 (1977).